

# Design and investigation of pentagonal shaped split ring resonator based microstrip patch antenna for high-speed terahertz applications

K. MAHENDRAN<sup>1,\*</sup>, SATHISH KUMAR DANASEGARAN<sup>2</sup>, R. INDHU<sup>3</sup>, S. ANNIE ANGELINE PREETHI<sup>3</sup>

<sup>1</sup>Department of ECE, Saveetha Engineering College, Thandalam, Chennai, 602105, India

<sup>2</sup>Centre for Advances in Signal Processing and Sensor Networks, Sri Eshwar College of Engineering, Coimbatore, 641202, India

<sup>3</sup>Department of ECE, Sathyabama Institute of Science and Technology (deemed to be university), Chennai 600119, India

Metamaterials have witnessed plentiful and quick development in the recent century as a primary strategy for manipulating electromagnetic (EM) waves. Metamaterials have developed adaptable and potent approaches for regulating EM waves and several novel applications that would be hard to accomplish with natural substances. Though metallic elements are commonly used to build metamaterials, nonmetallic elements may also be used. This article addressed the performances of a pentagonal split ring resonator (PSRR) based microstrip patch antenna (MPA) and the PSRR antenna is resonated at 1.4 THz. The antenna performances of the PSRR antenna are investigated by two different scenarios using computer simulation technology tool. In the first case, the structure of PSRR structure is varied for different angles such as 0°, 45°, 90°, 135°, 180°, 225°, 270° and 315°. The optimized PSRR structure is further analyzed by varying the split gap of the outer and inner pentagonal ring. With the influence of a dual-layer pentagonal ring, the patch antenna produces an excellent result of -61.97dB return loss, 1.000 VSWR, 6.75 dB of gain and 7.86 dB directivity. Hence, the proposed PSRR antenna is suitable for high-speed wireless applications and various THz devices.

(Received September 26, 2023; accepted April 10, 2024)

**Keywords:** Metamaterial, Microstrip patch antenna, Pentagonal split ring resonator, Terahertz frequency

## 1. Introduction

Telecommunications have become increasingly important in recent decades, and technology necessitates fast data transfer. Further studies are attempting to determine ways to boost the transmission rate in the range of terabytes per second (Tbps) region using various approaches in the THz [1-3] antenna. In the International Telecommunications Union (ITU), T waves are occupied from 0.03 to 3 mm and emit frequencies spanning 0.1 THz to 10 THz. T rays aid in effective data transmission of 1 Tbps. T waves' distinct features make them enticing for various technological, manufacturing, and healthcare applications. THz applications include wireless communications [4-7] with enormous bandwidth capacity, satellite linkages, airport security, bomb detection, material verification, remote sensing, and finding metallic & nonmetallic contaminants. THz imaging can detect liver and breast cancer in the medical field [8-11].

Antennas are a necessary component for every device in wireless technology. Several antenna models have been investigated to facilitate wireless communication at THz frequencies [5,8,10-26]. Among the investigation of various antenna structures, MPA's [12-16] emerged to be very appropriate in contrast to three-dimensional structures. Due to its affordable price, low profile, and ease of integration with THz devices. Furthermore, the MPA's main shortcoming is its narrow bandwidth, minimal gain, and signal band. These drawbacks can be overcome with the

impact of metamaterial structures. Also, THz antenna technology has advanced significantly as a result of the integration of metamaterials [17-20].

The artificial structure of metamaterial is employed in various wireless applications with the extended frequency range of THz. The antenna performances, like gain and bandwidth, are enhanced due to the property of a negative index. Metamaterials are made by organizing the tiny elements in an arrangement to achieve typical electromagnetic radiation or mechanical characteristics. Depending on their permittivity and permeability circumstances, the mediums can be categorized as  $\mu$ -negative, epsilon negative, or dual negative. Because of their versatility, metamaterial-based THz antennas have captured the interest of numerous researchers [21-23]. These antennas can also be used in biomedical devices like locating cancer cells, sensing haemoglobin, sugar, and urea levels, early recognition of tuberculosis, etc. Hence, THz antennas are required to achieve the fast rate and substantial gain specifications.

Pozar [24] suggested the patch and dipole structure with various substrates like gallium arsenide, quartz, and polytetrafluoroethylene for wireless communications. Yanbing et al. [25] reported the fractal structural dual-band metamaterial antenna for the applications of THz sensing. The author introduced the unique square Sierpinski fractal structure, which was more compact and had high sensitivity. The results demonstrate the sensors' high

sensitivity, indicating a wide range of terahertz sensing uses in biological and chemical sciences.

Radwan et al. [26] suggested the reconfigurable metamaterial antenna in which the antenna's operating frequency is varied by the voltage supplied. Further, the bandwidth and antenna radiation properties are improved by implanting the graphene-based SRR array in the structure. Abdelrehim et al. [27] investigated the patch antenna properties with the impact of left-handed metamaterials. The LH-MTM is positioned near the antenna's patch antenna, and because of its property of NRI, the radiation of the electromagnetic beam is decreased, providing a highly centered beam. The results show improved gain and directivity when the beamwidth is significantly reduced.

Bendaoudi et al. [28] studied the SRR antenna performances for different substrate materials like RT Duroid, Rogers RO 4232, and Bakelite. Based on the author's observation, all the substrate materials are appropriate for the S-band spectrum. Devapriya et al. [29] proposed the metamaterial rectangular patch antenna, which resonates at 1 THz. The suggested metamaterial antenna patch is very small at  $72 \times 95 \mu\text{m}^2$ , and the feed is  $39 \times 4.75 \mu\text{m}^2$ . The substrate of the antenna is chosen as quartz material for better antenna characteristics. The circular SRR (CSRR) unit cell is incorporated in the proposed structure in the array of  $3 \times 4$  with a radius of  $20 \times 15 \mu\text{m}^2$ . The SRR's size is the only factor that influences its resonance frequency. At the resonant frequency, the suggested CSRR exhibits a negative refractive index. As a result, negative permittivity and permeability are generated by the metamaterial with a gain of 5.75 dB.

Geetharamani et al. [30] proposed the THz antenna based on a metamaterial structure for detecting breast cancer cells. The perfect electric conductor material is utilized in the substrate layer, and the suggested metamaterial antenna resonated at 1 THz with a high gain value. The experiment was conducted twice in order to detect variations in the signal strength by examining the signal from tissue in the breast with as well as without a tumor. Althuwayb [31] investigated the on-chip antenna characteristics with the influence of metamaterial structure for various THz applications. The construction of the on-chip antenna is stacked with five polyimide layers, and the geometrical values are  $1000 \times 1000 \mu\text{m}^2$ . The obtained gain is varied from 1.1 to 1.8 dBi, and the efficiency is enhanced up to 60.50%. Babu et al. [32] proposed a tree-shaped MIMO patch antenna with the help of graphene material, and the substrate is made up of polyimide with a geometrical value of  $600 \times 300 \mu\text{m}^2$ . The proposed structure is ideal for short-distance data communication with fast connectivity and security scans.

Benkhallouk et al. [33] proposed a unique SRR patch antenna based on the Dodecagon structure. The approach used a technique of local field and enabled the collection of distinct negative-magnetic permeabilities dispersal properties. The proposed antenna utilized AD1000 substrate material to enhance the gain and directivity at 0.6 THz. The proposed Dodecagon model antenna is applicable for THz communication and imaging. Aggarwal et al. [34]

suggested a THz antenna with dual negative metamaterial superstrate for various THz applications. Constructing a nested rectangle ring metamaterial aims to enhance gain, bandwidth, and properties. The suggested antenna produces a RL of -24.0 dB, and the ratio of bandwidth is enhanced up to 26% at the operating frequency of 1.3 THz.

Olan et al. [35] designed and simulated the metamaterial antenna using called HFSS tool. The authors suggested the novel flower-shaped metamaterial structure along with silicon dioxide material. The magnetic field concentration in a silicon wafer is primarily eliminated by the flower unit cell, which also modifies the angle of electric and magnetic fields and curves them, mainly focused on and above the flower. Ashyap et al. [36] designed a multiband THz antenna using polyimide substrate and it is appropriate for the medical field. The geometrical value of the designed structure is  $600 \times 600 \times 0.25 \mu\text{m}^3$  and it is observed that the antenna's efficiency is improved up to 95.5%. Due to their dependability, affordability, and small footprint, multiband antennas have popularity in various applications. In contrast, single-band antennas require significant space for applications requiring more working frequencies.

Ajitha et al. [37] designed a miniaturized hexagonal SRR at 1.8 THz. This paper addressed the hexagonal SRR antenna characteristics with varying the thickness of hexagonal split thickness. The optimized hexagonal SRR antenna produced the excellent result of -44 dB RL, 6.4 dBi gain and the structure is suitable for high-speed wireless devices. Abdulkarem et al. [38] proposed four distinct MIMO antennae based on metamaterial resonating between 6 to 11 THz. Further, the investigation is carried out by varying the height of the  $\text{SiO}_2$  substrate and finding the optimized MIMO antenna structure. The THz patch antenna delivered higher bandwidth with a considerable gain value of 6.4 dB, whereas the CSRR patch antenna acquired a gain of 7.4 dB

Armghan et al. [39] analyzed a MIMO-based THz antenna and a metamaterial was used to design the MIMO antenna. A complimentary SRR patch is employed in the two-port antenna structure that is being suggested. The design outcomes are also contrasted with a straightforward patch antenna to demonstrate the antenna improvement. To enhance the antenna performance, the structure is optimized the substrate's thickness, the ground width, and the inner and outer ring width. Sivasangari et al. [40] suggested a THz antenna incorporated with hexagonal SRR for advanced wireless applications. This paper investigated the GaAs substrate material performances with the influence of hexagonal metamaterial structure. The electromagnetic features of metamaterials depend on the element configurations' regularity and size. The research gets furthered by varying the hexagonal ring thickness and slit width in the range of  $\mu\text{m}$ . The optimized hexagonal SRR structure delivered enhanced antenna performances such as -47 dB RL, 1.0008 VSWR and it is applicable for wireless [41-47] systems.

Based on the above research review, the primary difficulties are improving THz antenna efficiency and miniaturization. Most current research has demonstrated the

antenna characteristics of basic metamaterial structures like squares, rectangles, and circles with GHz antennas. Hence, this research proposed the promising model of a double-layer pentagonal metamaterial structure and explored the patch antenna characteristics by varying the pentagonal ring thickness and slit gap. The novelty of this paper is the patch antenna with dual hexagonal SRR structure and the antenna performance is analyzed from various angles. Moreover, the proposed antenna resonates at 1.4 THz, does not harm our human body and achieves an extreme data rate.

The organization of the manuscript is as follows, section 2 discusses the design of the proposed metamaterial antenna, and section 3 illustrates the impact of different angles of the pentagonal structure. The influence of the pentagonal ring slit gap is investigated in section 4 and section 5 concludes the manuscript.

## 2. Proposed design

The patch antenna comprises three distinct layers; the ground is the bottom of the structure, a patch is the topmost layer made up of copper and the substrate is the midlayer made up of polyimide material. The conventional patch antenna is designed using a computer simulation technology tool and illustrated in Fig. 1(a) and the pentagonal metamaterial structure is designed in two steps. The square patch is positioned above the polyimide substrate where the dielectric constant is 3.5 with a loss tangent of 0.02 and the inset feedline is utilized to design the MPA. The dimension of the substrate is  $65 \times 65 \mu\text{m}^2$  and the patch size is  $37.5 \times 37.5 \mu\text{m}^2$ . The functional frequency ( $f_{fr}$ ), height ( $h$ ) of the polyimide substrate, and dielectric constants ( $\epsilon_r$ ) are the key factors in designing the patch structure.  $P_{width}$  refers to width and  $P_{length}$  is the patch length of the structure.

$$P_{width} = \frac{c_0}{2f_{fr}} \sqrt{\frac{2}{\epsilon_r + 1}} \quad (1)$$

$$P_{length} = \frac{c_0}{2f_{fr} \sqrt{\epsilon_{reff}}} - 2\Delta L \quad (2)$$

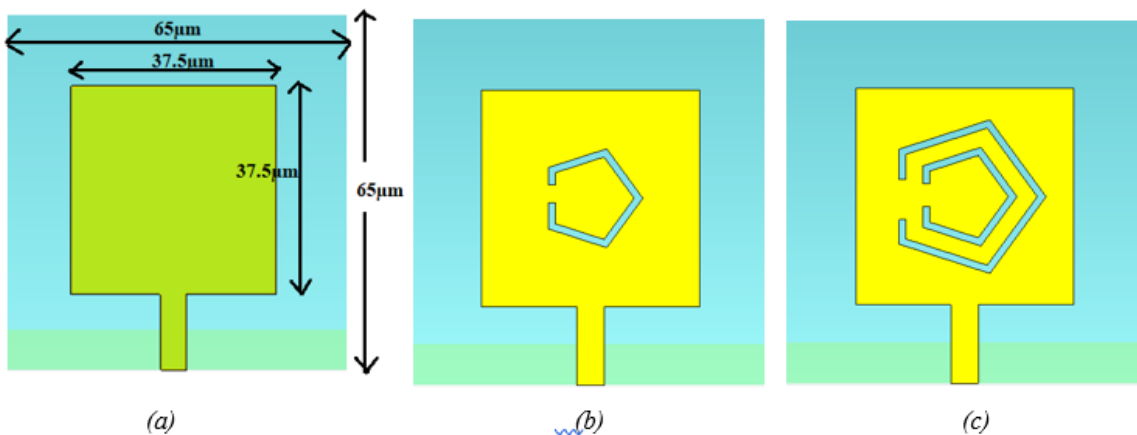


Fig. 1. Proposed antenna (a) conventional antenna (b) single pentagonal ring PSRR (c) double pentagonal ring PSRR (color online)  
Table 1. Performances of PSRR antenna at different angles

$$\epsilon_{reff} = \frac{\epsilon_r + 1}{2} + \frac{\epsilon_r - 1}{2} + \left[ 1 + 12 \frac{h}{P_{width}} \right]^{-1}, \frac{h}{P_{width}} > 1 \quad (3)$$

$$\epsilon_{eff} = \frac{\epsilon_r}{\sqrt{1 + \frac{12h}{f_{fr}}}} + 0.04 \left( 1 - \frac{f_{fr}}{h} \right)^2 \text{ if } \frac{f_{fr}}{h} < 1 \quad (4)$$

The dual pentagonal rings are incorporated into the conventional patch structure to enhance the antenna characteristics. Fig. 1 (b) shows the single pentagonal ring and Fig. 1 (c) displays the double pentagonal ring in the patch antenna.

## 3. Impact of various angles of pentagonal ring

In this section, the characteristics of the PSRR antenna are investigated by varying the angle of the pentagonal ring of the antenna model. The PSRR patch antenna comprises a dual pentagonal ring with a small slit gap. When the angle of the ring varies, it tends to influence the properties of electromagnetic waves in the antenna structure. Hence, the angle of the dual pentagonal ring is varied from  $0^\circ$  ( $360^\circ$ ) to  $315^\circ$  with a step angle of  $45^\circ$ . Based on the different angles of pentagonal rings, it is possible to design eight different PSRR structures, shown in Fig. 2 (a) to (h). All the designed PSRR structures are simulated and analyzed for antenna performances with the influences of various angles of the pentagonal rings. Table I listed the simulated antenna characteristics of the different angles of PSRR structures. Figure 3 illustrates the effect of return loss for various angles of PSRR structures. Fig. 4 (a) and (b) shows the effect of gain and directivity of the proposed PSRR structures. It is inferred that the pentagonal ring at an angle of  $180^\circ$  exhibits excellent antenna performances like  $-61.97$  dB return loss, 1.000 VSWR, 15.75 dBi gain, 16.86 dB directivity and this structure is considered to be an optimal PSRR.

Pentagonal ring angle (°)	Frequency (THz)	RL (dB)	VSWR	Gain (dBi)	Directivity (dB)	Bandwidth (THz)
0 or 360	1.462	-48.52	1.007	3.748	3.847	0.326
45	1.474	-24.69	1.123	3.628	3.741	0.276
90	1.475	-20.31	1.213	3.503	3.629	0.254
135	1.472	-26.61	1.097	3.663	3.779	0.295
180	1.457	-61.97	1.000	15.755	16.865	0.364
225	1.463	-24.44	1.127	3.576	3.693	0.251
270	1.486	-21.50	1.183	3.557	3.716	0.262
315	1.460	-26.54	1.098	3.599	3.718	0.301

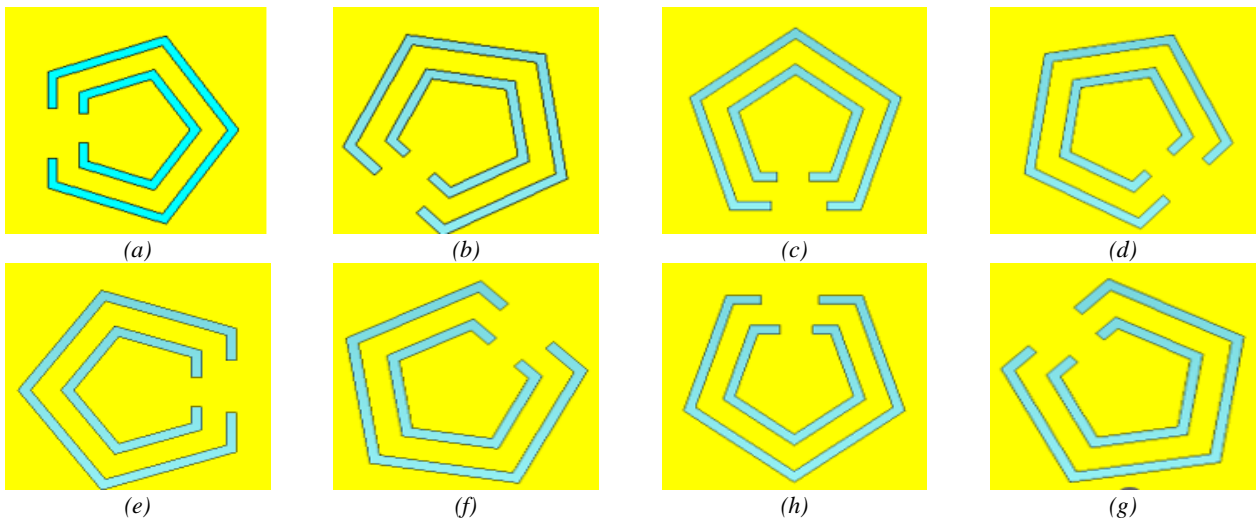


Fig. 2. Proposed PSRR antenna structures (a) 0° (b) 45° (c) 90° (d) 135° (e) 180° (f) 225° (g) 270° (h) 315° (color online)

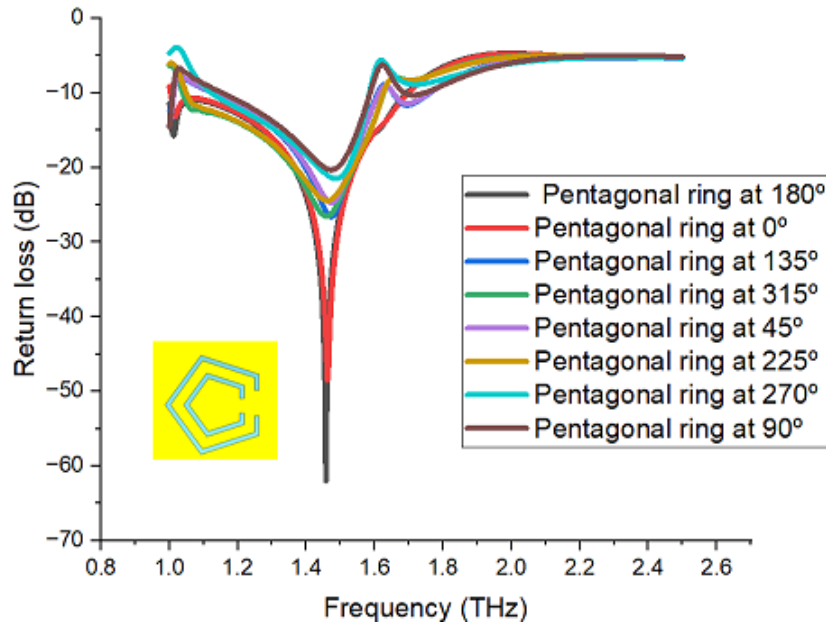


Fig. 3. Impact of return loss for various angles of PSRR rings (color online)

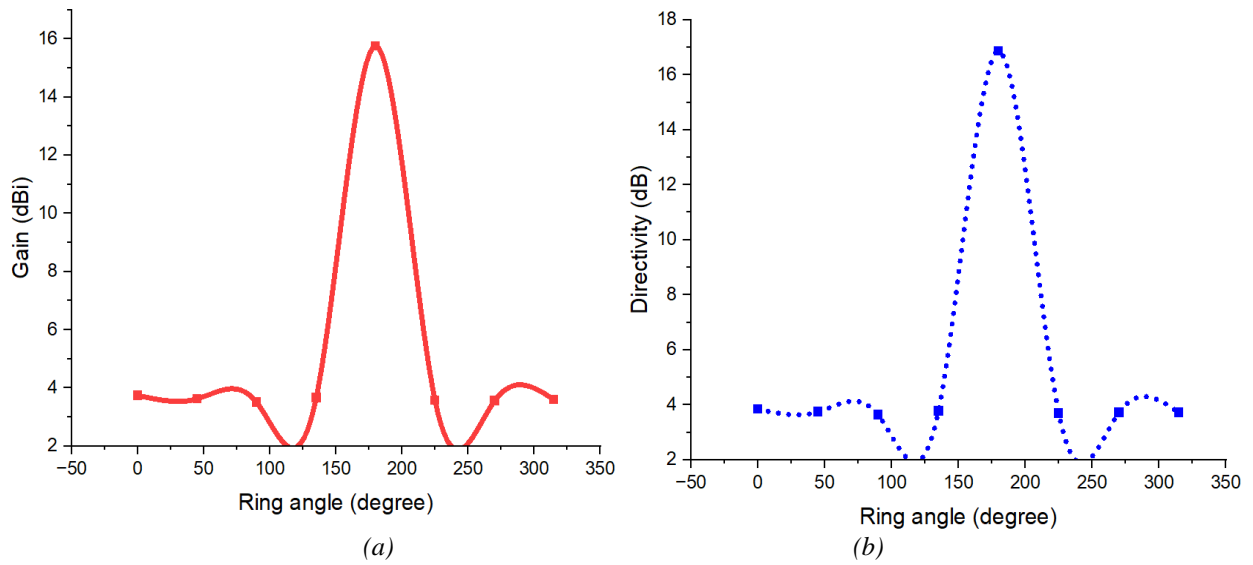


Fig. 4. Gain and directivity Vs pentagonal ring angle (color online)

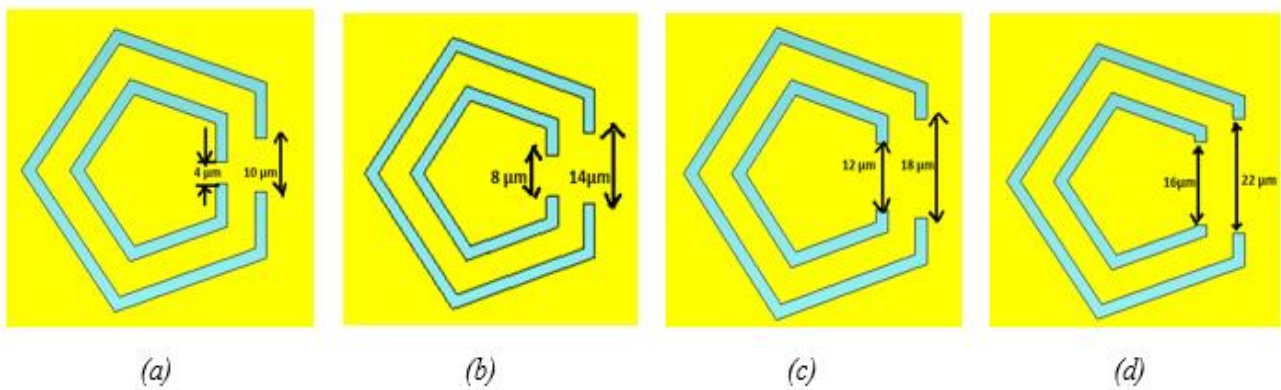


Fig. 5. Proposed PSRR for various slit gaps (a) 4  $\mu\text{m}$ , 10  $\mu\text{m}$  (b) 8  $\mu\text{m}$ , 14  $\mu\text{m}$  (c) 12  $\mu\text{m}$ , 18  $\mu\text{m}$  (d) 16  $\mu\text{m}$ , 22  $\mu\text{m}$  (color online)

Table 2. Performances of PSRR antenna for different slit gap

Slit gap of inner ring ( $\mu\text{m}$ )	Slit gap of outer ring ( $\mu\text{m}$ )	Frequency (THz)	RL (dB)	VSWR	Gain (dBi)	Directivity (dB)	Bandwidth (THz)
2	8	1.460	-35.86	1.032	3.794	3.981	0.289
4	10	1.456	-44.02	1.012	3.801	3.916	0.305
6	12	1.456	-48.68	1.007	3.774	3.879	0.317
8	14	1.457	-61.97	1.000	15.755	16.865	0.364
10	16	1.459	-46.82	1.009	3.739	3.837	0.328
12	18	1.460	-40.44	1.019	3.721	3.816	0.301
14	20	1.463	-36.70	1.029	3.711	3.805	0.287
16	22	1.463	-33.99	1.040	3.687	3.779	0.275

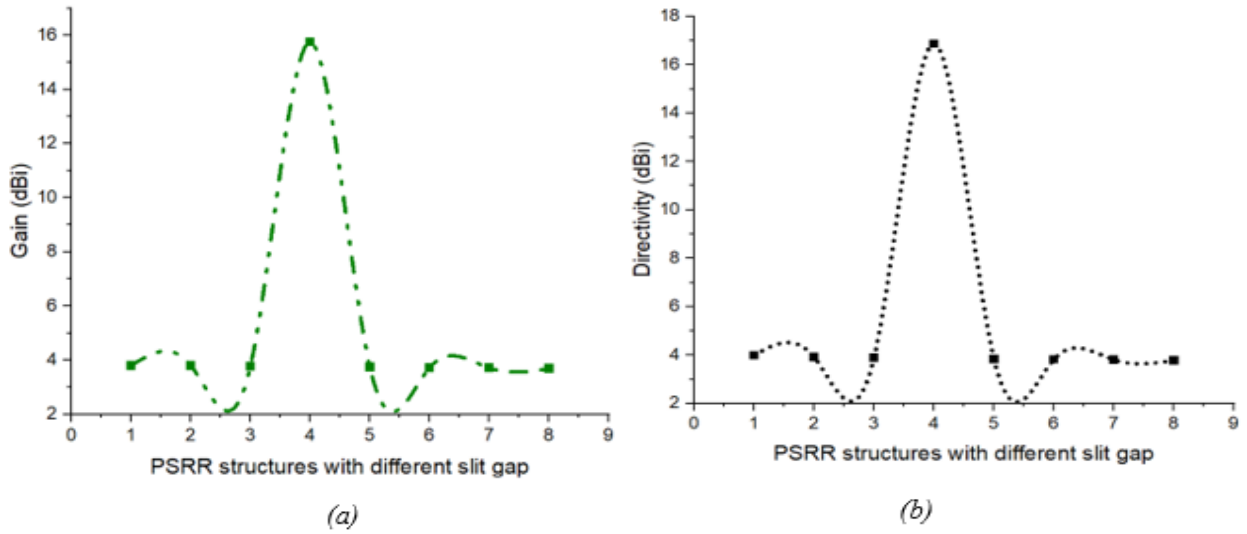


Fig. 6. Gain and directivity Vs pentagonal slit gap PSRR structures (color online)

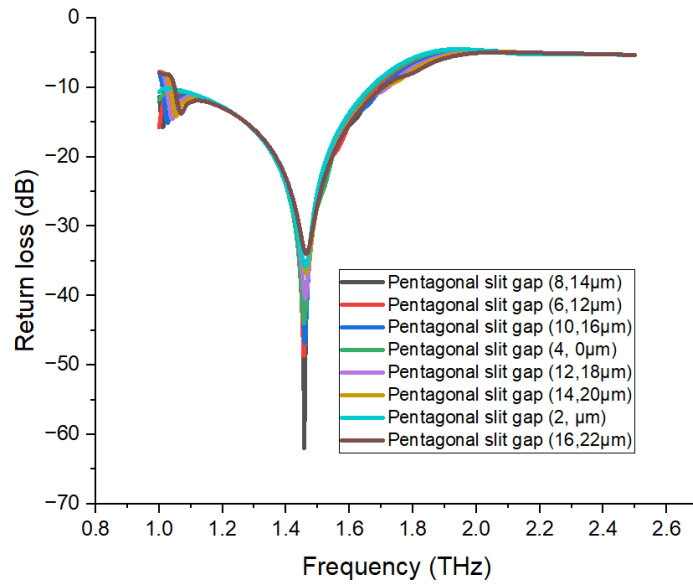


Fig. 7. Consequences of return loss for various ring angles

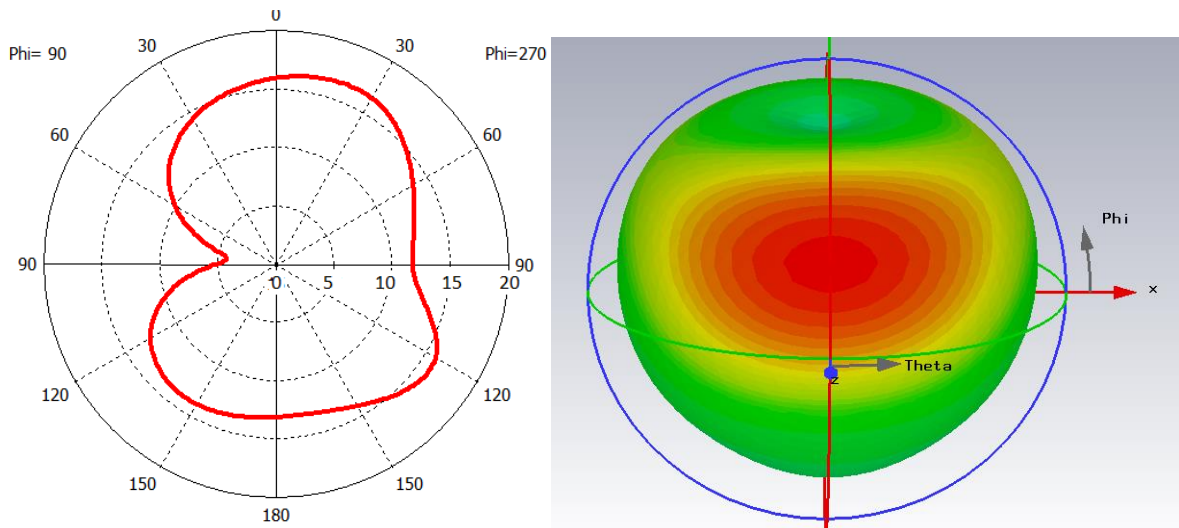


Fig. 8. Radiation plot of proposed TSRR antenna (a) 1D (b) 3D (color online)

Table 3. Contrast of proposed result with existing research papers

Parameters / Ref.	Substrate	Frequency (THz)	RL (dB)	VSWR	Gain (dBi)	Directivity (dB)
This work	Polyimide	1.457	-61.97	1.000	15.755	16.865
Olan et al. [35]	Silicon	0.81	-40.79	> 1	6.5	>6
Ajitha et al. [37]	Roger 4350	1.816	-44.02	1.012	6.471	>7
Sivasangari et al. [40]	GaAs	1.992	-47.09	1.0088	8.649	8.696
Britto et al. [43]	Roger 5880	2.02	>-40	1.0046	8.716	8.730
Kiani et al. [45]	Silicon dioxide	0.587	> - 10	> 1	--	--
Dave et al. [46]	Roger 5880	15.2	-48	> 1	11	> 10

#### 4. Consequence of various pentagonal ring slit gap

Based on the investigation of the prior sections, the PRSS patch antenna produces the optimal result at the pentagonal ring with an angle of  $180^\circ$ . This section examines the antenna properties of optimized PSRR by fluctuating the slit gap of the inner ring varies from 2 to 16  $\mu\text{m}$  and the outer ring gap is varied from 8 to 22  $\mu\text{m}$ . On the basis of various split gaps, this section presents eight different PSRR structures, and the sample PSRR structures are shown in Fig. 5 (a) to (d). The proposed PRSS structures are simulated and the results are shown in Table 2. Fig. 6 (a) and (b) illustrate the impact of gain and directivity for the proposed PRSS structures. Fig. 7 shows the comparison plot of RL for various pentagonal split gaps. Fig. 8 (a) depicts the 1D curve of the proposed PSRR model's and proving that the central lobe magnitude is higher at the angle of  $30^\circ$  than side lobe radiation. The 3D radiation plot is shown in Fig. 8 (b) and the directivity is obtained as 16.856 dB. It is observed that the PSRR structure with an inner split gap of 8  $\mu\text{m}$  and an outer ring gap of 14  $\mu\text{m}$  offers outstanding antenna properties.

This paper investigates the antenna characteristics at two distinct scenarios a) PSRR structure for different angles and b) PSRR structure for different inner and outer ring width. Each case produces the antenna performance based on the designed structure, especially second case yields excellent RL performances for all proposed designs. It is inferred that the intended signal will reach the receiver without getting back to the transmitter.

#### 5. Comparison of proposed PSRR with existing works

The proposed PSRR antenna result is compared with the existing research works and listed in Table 3. It is observed that the PSRR antenna outperforms prevailing works. The RL of the proposed PSRR model is -61.97 dB, demonstrating that the strength of the signal is powerful. The PSRR directivity is 16.86 dB, which assists in directing

signal to the targeted direction. The proposed PSRR antenna's substantial gain strengthens radio transmission accuracy, particularly for long-distance network connections. The bandwidth of the proposed PSRR antenna is 0.364 THz which facilitates fast data communication and an outstanding data rate in wireless technologies.

There are numerous difficulties in fabricating the proposed THz antenna which involves design specifications, material choices and performance attributes. The PSRR antenna resonates at 1.457 THz necessitating progressed approaches and equipment. Hence, the prototype gadgets were not included in this work but may be carried out in the future depending on available resources for THz antenna fabrication.

#### 6. Conclusion

This paper demonstrates that the PSRR metamaterials antenna influences the potent electromagnetic waves and will play a significant role in modern wireless devices. The proposed dual pentagonal SRR antenna is miniaturized and resonating at a frequency of 1.45 THz. Further, the performances of the PSRR structure are investigated in two ways by varying the angle of pentagonal rings and modifying the slit gap of the rings. The simulated result of the optimized PSRR antenna is a -61.97 dB return loss with a gain of 15.75 dBi. The investigation results establish the groundwork for potential improvements in wireless communication technologies with fast data rates and motivate forthcoming research endeavors in reconfigurable antennas.

#### References

- [1] T. Robin, C. Bouye, J. Cochard, Proc. SPIE **8985**, Terahertz, RF, Millimeter, and Submillimeter-Wave Technology and Applications **VII**, 898512 (2014).
- [2] A. Y. Pawar, D. D. Sonawane, K. B. Erande, D. V. Derle, Drug Invention Today **5**, 157 (2013).

- [3] I. F. Akyildiz, J. M. Jornet, C. Han, *Physical Communication* **12**, 16 (2014).
- [4] A. Sharma, V. K. Dwivedi, G. Singh, *Progress in Electromagnetics Research Symposium, Beijing, China*, 627 (2009).
- [5] Y. M. Ding, S. Gao, X. Shi, H. Wu, *3rd International Conference on Wireless Communication and Sensor Network (WCSN 2016)* 44, 180 (2016).
- [6] S. Lalithakumari, S. K. Danasegaran, G. Rajalakshmi, R. Pandian, E. C. Britto, *Brazilian Journal of Physics* **53**, 140 (2023).
- [7] R. Pandian, S. K. Danasegaran, Lalitha Kumari, G. Rajalakshmi, G. Sathish Kumar, *Optical and Quantum Electronics* **56**(5), 763 (2024).
- [8] S. Rahmatinia, B. Fahimi, *IEEE Trans. Magn.* **53**(6), 1 (2017).
- [9] M. Bassi, M. Caruso, M. S. Khan, A. Bevilacqua, A.-D. Capobianco, A. Neviani, *IEEE Trans. Microw. Theory Tech.* **61**(5), 2108 (2018).
- [10] E. Porter, M. Coates, M. Popovic, *IEEE Transactions on Biomedical Engineering* **63**(3), 530 (2016).
- [11] M. Asili, P. Chen, A. Z. Hood, A. Purser, R. Hulsey, L. Johnson, E. Topsakal, *IEEE Antennas and Wireless Propagation Letter* **14**(7), 1778 (2015).
- [12] D. S. Kumar, S. Poonguzhali, A. Sivasangari, S. Lalithakumari, G. Rajalakshmi, R. Pandian, *International Conference on System, Computation, Automation and Networking (ICSCAN), Puducherry, India*, 1-5 (2023).
- [13] M. Nahas, *Journal of Radiation Research and Applied Sciences* **15**(4), 100483 (2022).
- [14] D. S. Kumar, S. Pavithra, K. S. Ranjith, R. Kiruthika, E. Kavin, *7th International Conference on Electronics, Communication and Aerospace Technology (ICECA), Coimbatore, India*, 1464 (2023).
- [15] C. M. Krishna, S. Das, A. Nella, S. Lakrit, B. Madhav, *Plasmonics* **16**, 2167 (2021).
- [16] Sathish Kumar Danasegaran, Elizabeth Caroline Britto, K. Sagadevan, M. Paranthaman, S. Poonguzhali, Mahendran Krishna Kumar, *Brazilian Journal of Physics* **54**, 31 (2024).
- [17] S. Roy, U. Chakraborty, *IET Communications* **12**, 1448 (2018).
- [18] M. K. Khandelwal, B. K. Kanaujia, S. Kumar, A. K. Gautam, *Microwave and Optical Technology Letters* **59**(4), 862 (2017).
- [19] M. Alibakhshikenari, B. S. Virdee, D. Mariyanayagam, D. Vadala, V. Moghadasi, M. N. C. See, I. Dayoub, S. Aissa, P. Livreri, S. H. Burokur, A. P. Dabrowska, F. Falcone, S. Koziel, E. Limiti, *Scientific Reports* **12**, 17893 (2022).
- [20] L. Choi W. Zhang, *IEEE Antennas and Wireless Propagation Letters* **17**, 1478 (2018).
- [21] B. Danana, B. Choudhury, R. M. Jha, *Electron. Instrument. Eng.* **3**(5), 711 (2014).
- [22] S. Singhal, *Microw. Opt. Technol. Lett.* **61**, 2366 (2019).
- [23] Y. Denizhan Sirmaci, C. K. Akin, C. Sabah, *Optical and Quantum Electronics* **48**, 168 (2016).
- [24] D. M. Pozar, *IEEE Transactions on Antennas and Propagation* **31**(5), 740 (1983).
- [25] Yanbing Ma, Huai-Wu Zhang, Yuanxun Li, Yicheng Wang, Weien Lai, *Progress In Electromagnetics Research* **138**, 407 (2013).
- [26] Radwan, M. D'Amico, G. G. Gentili, V. Verri, *9th European Conference on Antennas and Propagation (EuCAP), Lisbon, Portugal*, 1 (2015).
- [27] A. A. A. Abdelrehim, H. Ghafouri-Shiraz, *Microwave and Optical Technology Letters* **58**, 382 (2016).
- [28] A. Bendaoudi, Z. Mahdjoub, *Photonic Network Communications* **35**, 195 (2018).
- [29] Amalraj Devapriya, Savarimuthu Robinson, *Journal of Microwaves, Optoelectronics and Electromagnetic Applications* **18**, 377 (2019).
- [30] G. Geetharamani, T. Aathmanesan, *SN Applied Sciences* **1**, 595 (2019).
- [31] Ayman A. Althwayb, *International Journal of Antennas and Propagation* **2020**, 6653095 (2020).
- [32] K. Vasu Babu, Sudipta Das, Gaurav Varshney, S. J. N. Gorre, B. T. P. Madhav, *Journal of Computational Electronics* **21**, 1 (2022).
- [33] K. Benkhallouk, A. Bendaoudi, M. Berka, Z. Mahdjoub, *Journal of Engineering and Applied Science* **69**, 71 (2022).
- [34] I. Aggarwal, S. Pandey, M. R. Tripathy, A. Mittal, *Journal of Electronic Materials* **51**, 4589 (2022).
- [35] K. N. Olan-Nuñez, R. S. Murphy-Arteaga, *Scientific Reports* **12**, 1699 (2022).
- [36] Adel Ashyap, A. A. Shamsan, Muhammad Inam Abbasi, M. R. Kamarudin, Muhammad Dahri, K. Almuhan, F. Alorifi, *Computers, Materials and Continua* **74**, 1765 (2022).
- [37] Ajitha Ponnupillai, Arunakiri Sivasangari, Sathish Kumar Danasegaran, Somasundaram Poonguzhali, Immanuel Rajkumar, *International Journal of Communication Systems* **36**(7), e5454 (2023).
- [38] Abdulkarem H.M. Almagani, Shobhit K. Patel, Truong Khang Nguyen, Anwar A. H. Al-Athwary, *Optik* **287**, 171054 (2023).
- [39] A. Armghan, K. Aliqab, M. Alsharari, O. Alsalmán, J. Parmar, S. K. Patel, *Micromachines* **14**, 1328 (2023).
- [40] D. Deepa Sivasangari, P. Ajitha, R. M. Gomathi, R. Vignesh, Sathish Kumar Danasegaran, S. Poonguzhali, *Journal of Electronic Materials* **52**, 4785 (2023).
- [41] A. Bharadwaj, S. Vincent, T. Ali, *Optik* **272**, 170335 (2023).
- [42] R. Pant, L. Malviya, *Int. J. Commun. Syst.* **36**(8), e5474 (2023).
- [43] E. C. Britto, S. K. Danasegaran, K. Sagadevan, *Metamaterial Technology and Intelligent Metasurfaces for Wireless Communication Systems*, S. Mehta and A. Abougreen (Eds.) 180 (2023).
- [44] C. Mustacchio, L. Boccia, E. Arneri, G. Amendola,

- Proceedings of the 50th European Microwave Conference (EuMC), 650 (2021).
- [45] N. Kiani, F. Tavakkol Hamedani, P. Rezaei, *Optical and Quantum Electronics* **55**(4), 101007 (2023).
- [46] K. Dave, V. Sorathiya, S. Lavadiya, S. K. Patel, U. Dhankecha, D. Swain, O. S. Faragallah, M. M. A. Eid, A. N. Z. Rashed, *Appl. Phys. A* **128**(8), 656 (2022).
- [47] K. Mahendran, H. Sudarsan, S. Rathika, *AEUE - International Journal of Electronics and Communications* **161**, 154543 (2023).

---

\*Corresponding author: [srimahendrancs@gmail.com](mailto:srimahendrancs@gmail.com)